

# A Born–Green–Yvon integral equation treatment of a compressible fluid

J. E. G. Lipson<sup>a)</sup> and S. S. Andrews

Department of Chemistry, Dartmouth College, Hanover, New Hampshire 03755

(Received 5 August 1991; accepted 2 October 1991)

Previous work using the Born–Green–Yvon (BGY) integral equation approach has been extended to investigate the case of a pure compressible lattice fluid, yielding the equation of state as our main result. We show that the BGY equation does a very good to excellent job at fitting the experimental pressure–volume–temperature surface for both small molecules and polymers; the fit parameters are then used to make predictions about thermodynamic properties for the system of interest. We note that two other equations of state can easily be obtained from the BGY equation, and compare results using BGY and other equations of state. We also comment on the agreement between the BGY description in the athermal limit, which is equivalent to Guggenheim’s treatment of random mixing, and some lattice Monte Carlo results.

## I. INTRODUCTION

In previous work<sup>1,2</sup> one of us (J. E. G. L.) has outlined the theoretical treatment of a binary, incompressible lattice mixture using the Born–Green–Yvon integral equation approach. It has been shown how the thermodynamic description of such a system could be derived analytically, and the BGY results have been compared with those from simulation studies and other lattice theories. The next goal in this work involves extending the lattice model to the case of a compressible mixture; at that stage comparison with experimental results and with treatments incorporating free volume effects will become possible. In doing so, it will be necessary to use information characteristic of the pure components; typically such information is obtained by fitting experimental pressure–volume–temperature (PVT) data to an equation of state derived for the pure component, in order to extract “characteristic parameters.” Different choices for the three parameters can be used, but a common set is the nonbonded nearest-neighbor interaction energy,  $\epsilon$ , the number of contiguous lattice sites occupied per chain,  $r$ , and the volume associated with a lattice site,  $\nu$ . Before proceeding to the case of a compressible mixture, it is important to study the compressible pure fluid problem, and that is the focus of the present study.

Among the questions to be answered here are: Can the BGY theory yield a good fit to experimental PVT data? Can it predict a liquid–vapor transition? Can the fit parameters be used to predict other thermodynamic properties? Finally, how does this description compare with other equations of state? Many such equations have been obtained, and some of these have been very successful at describing pure fluids. The questions listed here are addressed in the following manner: In Sec. II the BGY theory is used to derive the equation of state for a compressible fluid. In Sec. III the equation is ex-

pressed in reduced variables along with other equations of state to be compared with BGY. In Sec. IV the athermal version of the BGY result, which is equivalent to Guggenheim’s treatment of random mixing,<sup>3,4</sup> is compared with lattice simulation results, and in Sec. V the complete BGY equation of state is applied to experimental data on  $n$ -alkanes and several polymers, and the results are compared with those using the equations listed in Sec. III. Our conclusions are discussed in Sec. VI.

## II. THE EQUATION OF STATE FOR A COMPRESSIBLE PURE FLUID

We model the compressible fluid as a mixture of  $rN$  occupied lattice sites, and  $N_h$  unoccupied sites, or holes; we imagine the occupied sites to be connected such that  $r$  contiguous sites are associated with a molecule. The fractions of occupied and unoccupied sites are denoted  $\phi$  and  $\phi_h$ , respectively, where

$$\phi = rN / (rN + N_h), \quad \phi_h = N_h / (rN + N_h). \quad (1)$$

The interaction energy associated with nonbonded nearest-neighbor segments is  $\epsilon$ ; the empty sites do not contribute towards the total potential energy of the system. As in the study of incompressible mixtures,<sup>1</sup> we also define a concentration variable which accounts for the nearest-neighbor connectivity of the molecules,

$$\xi = qN / (qN + N_h), \quad \xi_h = N_h / (qN + N_h), \quad (2)$$

where

$$qz = rz - 2r + 2. \quad (3)$$

$z$  is the lattice coordination number and  $rz$  is the number of nearest-neighbor contacts associated with  $r$  disconnected (and separated) segments;  $qz$  is the maximum number of nearest-neighbor contacts for a linear chain having  $r$  segments. Hence the use of  $\xi$  incorporates to some extent the effects of chain connectivity in the molecule. Here we assume that the smallest unit of free volume in the lattice is that associated with one lattice site.

Using the results of Ref. 2, the change in internal energy associated with mixing  $N$   $r$ -mers with  $N_h$  holes is given by

<sup>a)</sup> Author to whom correspondence should be addressed.

$$\frac{\beta \Delta E_{\text{mix}}(T)}{N_0} = (z/2)(q/r)\beta\epsilon\phi \times \left( \left\{ \frac{\xi \exp(-\beta\epsilon)}{[\xi \exp(-\beta\epsilon) + \xi_h]} \right\} - 1 \right), \quad (4)$$

where  $\beta = 1/k_B T$  and  $N_0$  is the total number of lattice sites. This result is obtained using Eq. (14) of Ref. 2 with  $\epsilon_{11} = \epsilon_{12} = 0$ , and  $\epsilon_{22} = \epsilon$ . In deriving an expression for the Helmholtz energy of the fluid we make use of the Gibbs-Helmholtz relationship

$$E = \frac{\partial(A/T)}{\partial(1/T)} \Big|_{\nu} \quad (5)$$

and take the lower limit of the integration (i.e.,  $T$  approaches infinity) to be associated with the free energy of a pure fluid with holes randomly distributed throughout the lattice. Thus we approximate the athermal free energy by an estimate for the free energy associated with ‘‘randomly mixing’’ the holes and segments; in particular, the expression developed by Guggenheim<sup>4</sup> (denoted GRM for Guggenheim random mixing) is used here

$$\frac{-\Delta S(\text{GRM})}{N_0 k_B} = \phi_h \ln \phi_h + (\phi/r) \ln \phi + (z/2) \times [\phi_h \ln(\xi_h/\phi_h) + (q/r)\phi \ln(\xi/\phi)]. \quad (6)$$

Putting together Eqs. (4) through (6), the free energy change associated with mixing the holes and segments to form a compressible fluid at temperature  $T$  is given by

$$\frac{\beta \Delta A_{\text{mix}}}{N_0} = -\frac{qz\phi}{r} \ln[\xi \exp(-\beta\epsilon) + \xi_h] + \left\{ \phi_h \ln \phi_h + \frac{\phi}{r} \ln \phi + \frac{z}{2} \left[ \phi_h \ln \left( \frac{\xi_h}{\phi_h} \right) + \frac{q}{r} \phi \ln \left( \frac{\xi}{\phi} \right) \right] \right\}. \quad (7)$$

This result can be used to obtain the equation of state, since

$$P = -\frac{\partial A}{\partial V} \Big|_T \quad (8)$$

Using Eqs. (7) and (8) we find

$$P = -\frac{1}{\beta\nu} \left\{ \ln \phi_h + \frac{z}{2} \ln \left( \frac{\xi_h}{\phi_h} \right) + \phi \left( 1 - \frac{1}{r} \right) + \frac{z}{2} \phi \left( \frac{q}{r} - 1 \right) + \frac{z}{2} \xi^2 \left[ \frac{\exp(-\beta\epsilon) - 1}{\xi \exp(-\beta\epsilon) + \xi_h} \right] \right\}, \quad (9)$$

where  $\nu$  is the volume per lattice site. Given the definition of  $q$  from Eq. (3) it can be seen that, unless  $q$  is set equal to  $r$  (if nearest-neighbor connectivity is neglected, or if  $r = 1$ ), the third and fourth terms on the right-hand side of Eq. (9) will cancel. Equation (9) is the central result of this paper. In the following section we will express the equation of state in reduced variables and compare our result with those of several other theoretical treatments.

### III. COMPARISON IN REDUCED VARIABLES OF THE BGY RESULT WITH OTHER EQUATIONS OF STATE

It is usual to express an equation of state, such as Eq. (9), in reduced variables. Here we shall mainly follow the notation of Sanchez and Lacombe<sup>5</sup> in writing four of the five equations to be used. The four equations other than BGY are: the lattice fluid model (LF) derived by Sanchez and Lacombe,<sup>5</sup> the lattice cluster (LC) model,<sup>6</sup> using the polymer equation of state which was developed by Bawendi and Freed,<sup>7</sup> the result obtained by Panayiotou and Vera<sup>8</sup> (PV) using some concepts introduced by Guggenheim,<sup>3</sup> and the Simha-Somcynsky<sup>9</sup> (SS) equation. It is difficult to find notation which is equally suited to expressing all of these equations in reduced form; for example, the LF notation is not convenient for writing the Simha-Somcynsky result in that it would make their equation artificially complex (and unfamiliar). The reduction parameters for the other equations are given by

$$\begin{aligned} \tilde{T} &\equiv T/T^*, & T^* &\equiv z\epsilon/2k_B, \\ \tilde{P} &\equiv P/P^*, & P^* &\equiv z\epsilon/2\nu. \end{aligned} \quad (10)$$

Sanchez and Lacombe<sup>5</sup> use  $\rho$ , where we have used  $\phi$ ; we will continue using both  $\phi$  and  $\xi$  as our dimensionless concentration variables. In reduced form the BGY equation of state becomes

$$\tilde{P} + \tilde{T} [\ln(1 - \phi) - (z/2) \ln[(1 - \phi)/(1 - \xi)]] + (1 - 1/r)\phi\delta_{q,r} + (z/2)J\xi^2 = 0, \quad (11)$$

where  $\delta_{q,r}$  is the Kronecker delta, and  $J$  is given by

$$J = [\exp(-2/z\tilde{T}) - 1]/[\xi \exp(-2/z\tilde{T}) + (1 - \xi)]. \quad (12)$$

The presence of the term with the Kronecker delta is related to the discussion above regarding the third and fourth terms in Eq. (9). The LF equation of state<sup>5</sup> is

$$\tilde{P} + \tilde{T} [\ln(1 - \phi) + (1 - 1/r)\phi] + \phi^2 = 0. \quad (13)$$

The LF result can be obtained from the BGY result by setting  $q = r$  (therefore  $\xi = \phi$ ) and by expanding  $J$  and keeping only terms to  $O(\beta\epsilon)$ . The PV equation of state<sup>8</sup> is

$$\tilde{P} + \tilde{T} [\ln(1 - \phi) - (z/2) \times \ln[(1 - \phi)/(1 - \xi)]] + \xi^2 = 0. \quad (14)$$

The PV result can be obtained from the BGY result by expanding  $J$  to  $O(\beta\epsilon)$ . Note that the appearance of  $\xi$ 's implies that  $q \neq r$ . Thus the LF and PV results are obtained as simplified versions of the BGY result. The above three equations retain a formal dependence on  $r$ , both in the term associated with the factor or  $1/r$  (BGY and LF) and in the presence of  $\xi$  (BGY and PV).  $\xi$ , defined in Eq. (2), can also be written as

$$\xi = \phi/[\phi + (r/q)(1 - \phi)]. \quad (15)$$

As  $r$  becomes very large,  $r/q \rightarrow z/(z - 2)$  and so all equations are expected to obey a corresponding states principle for the polymer case. The LC equation of state for polymers<sup>6</sup> is given by

$$\begin{aligned} \bar{P} + \bar{T} [\ln(1 - \phi) + \phi + \phi^2(1/\bar{T} - 4/\bar{T}z + 1/z\bar{T}^2 \\ + 1/z + 3/z^2) + \phi^3(4/\bar{T}z - 4/\bar{T}^2z - 20/3z^2) \\ + \phi^4(3/\bar{T}^2z + 6/z^2) \\ + O[N^{-1}, z^{-3}, 2\bar{T}^{-1}z^{-2}, 4(\bar{T}z)^{-2}]] = 0. \end{aligned} \quad (16)$$

Finally, the SS equation of state<sup>9</sup> is given by

$$\begin{aligned} \tilde{P}'\tilde{V}'/\tilde{T}' = [1 - 2^{-1/6}y(\tilde{V}')^{-1/3}]^{-1} \\ + (2y/\tilde{T}')(\tilde{V}')^{-2} \\ \times [1.011(y\tilde{V}')^{-2} - 1.2045], \end{aligned} \quad (17a)$$

where the primes serve as reminders that the reduction parameters are different for the SS equation.  $y$  is the fraction of occupied sites, depending here on  $r$  and on an additional parameter,  $c$ , defined such that there are  $3c$  external degrees of freedom per chain. Here the reduced variables are

$$\tilde{V}' = V/Nrv^*; \quad \tilde{T}' = c/(qz\beta\epsilon); \quad \tilde{P}' = Prv^*/qz\epsilon, \quad (17b)$$

where  $v^*$  is the characteristic volume per segment of the chain.

#### IV. COMPARISONS WITH OTHER EQUATIONS OF STATE AND MONTE CARLO RESULTS FOR ATHERMAL MELT

In the athermal limit ( $\epsilon = 0$ ) the BGY description reduces to the GRM equation of state.<sup>3</sup> Dickman and Hall, working both together<sup>10,11</sup> and separately,<sup>12,13</sup> have studied athermal chains. Most of what follows will reference Monte Carlo (MC) data on lattice chains;<sup>13</sup> a comment related to some of the continuum results<sup>11</sup> will appear in Sec. VI.

In making comparison with the simulation data there are two quantities of interest. One is the insertion probability,  $p(\phi, r)$ , which is the probability that a randomly chosen  $r$ -mer, placed at random into a randomly chosen configuration of  $N$   $r$ -mers on a lattice of  $N_0$  sites, will not overlap with any of the other chains on the lattice.<sup>10</sup> As Bawendi and Freed noted,<sup>7</sup> this can be easily obtained once an expression for the free energy of the system is known. The result for GRM is

$$\begin{aligned} (l/r) \ln p(\phi, r) = \ln(1 - \phi) \\ - [(r - 1)/r] \ln[(1 - \phi)/(1 - \xi)]. \end{aligned} \quad (18)$$

This can be compared with the Flory–Huggins (FH) result, which would include only the first term on the right-hand side, and with the LC result of Ref. 7.<sup>14</sup> Monte Carlo results are available in both two and three dimensions. Figure 1 from Ref. 13(a) shows data for a simple cubic lattice, and illustrates the difference in the three theoretical predictions for chains of length 5, 10, and 20 segments. It is important to note that what we (and others) denote “Flory–Huggins,” Hertanto and Dickman<sup>13</sup> call “Flory;” they refer to GRM as “Flory–Huggins.” For  $r = 5$  both the GRM and LC theories agree extremely well with the MC predictions; this is also true for  $r = 10, 20$ , but the LC equation does marginally better for the longest chain length. This may be because GRM accounts for connectivity only with respect to nearest-neighbors, while LC is supposed to incorporate longer-range

effects. For the case of thermodynamic properties where interactions are only counted to nearest-neighbor, the two have been shown to agree even more closely, for some cases.<sup>15</sup> Note that FH does rather poorly over the entire concentration range, even for low chain lengths.

A quantity of greater practical interest is the compressibility factor,  $\omega$ , defined as

$$\omega = PV_m/RT = Prv/\phi RT. \quad (19)$$

Once an expression for the equation of state is obtained it is straightforward to work out the result for the compressibility factor. For GRM this is

$$\begin{aligned} \omega_{\text{GRM}} = 1 - (r/\phi)[\phi + \ln(1 - \phi)] \\ + (zr/2\phi) \ln[(1 - \phi)/(1 - \xi)] + (r - 1). \end{aligned} \quad (20)$$

The result using FH,  $\omega_{\text{FH}}$ , is given by the first three terms on the right-hand side of Eq. (20).<sup>16</sup> Figure 1 from Ref. 13(b) shows several sets of Monte Carlo data for the simple cubic lattice, along with the predictions using the GRM, FH, and LC equations, combining results from simulations in which the chain length was fixed at  $r = 40$  with those in which there was a uniform or bimodal distribution of chain lengths about an average of  $r = 40$ . It is interesting that these simulation data would seem to indicate that there is little (if any) effect on the compressibility factor of having these kinds of molecular weight distributions. The theoretical results were all obtained using  $r = 40$ . FH is consistently higher than the simulation results, but does show the correct curvature. At low densities LC is a little closer to the simulation results, but at higher densities LC and GRM are indistinguishable. Taking the case of a chain with  $r = 40$ , and approximating the volume of a lattice site to be about  $(.009/N_{\text{avo}})L/\text{mol}$ , where  $N_{\text{avo}}$  is Avogadro's number, volume fractions of 0.2 and 0.8 would correspond to molar volumes of about 1.8 and 0.45 L, respectively. Thus the liquid regime will be associated with values of  $\phi$  close to 1, and in this region GRM is in excellent agreement with the simulation results.

#### V. COMPARISON WITH EXPERIMENTAL DATA AND OTHER EQUATIONS OF STATE

Referring to the questions raised in Sec. I, we shall first investigate how well the BGY equation of state can fit experimental PVT data and compare our results to those using other theoretical approaches. We can also consider, for small molecule fluids, the ability of BGY to predict a liquid–vapor transition. In addition, other thermodynamic properties such as the thermal expansion coefficient will be of some interest. In the first portion of this section we shall focus on  $n$ -alkanes, and will then examine several polymeric systems.

Since there are comprehensive PVT data sets available for the homologous linear alkanes<sup>17</sup> we chose to study a series having between four and twenty carbons per molecule. Figure 1 shows the BGY fit to a series of isotherms for  $n$ -C5 (pentane),  $n$ -C10 (decane), and  $n$ -C20 (eicosane). The results were obtained by fitting the experimental PVT surface for the liquid [using Eq. (9)] thus determining best values for the three parameters  $\nu$ ,  $\epsilon$ , and  $r$ , while keeping  $z$  fixed.

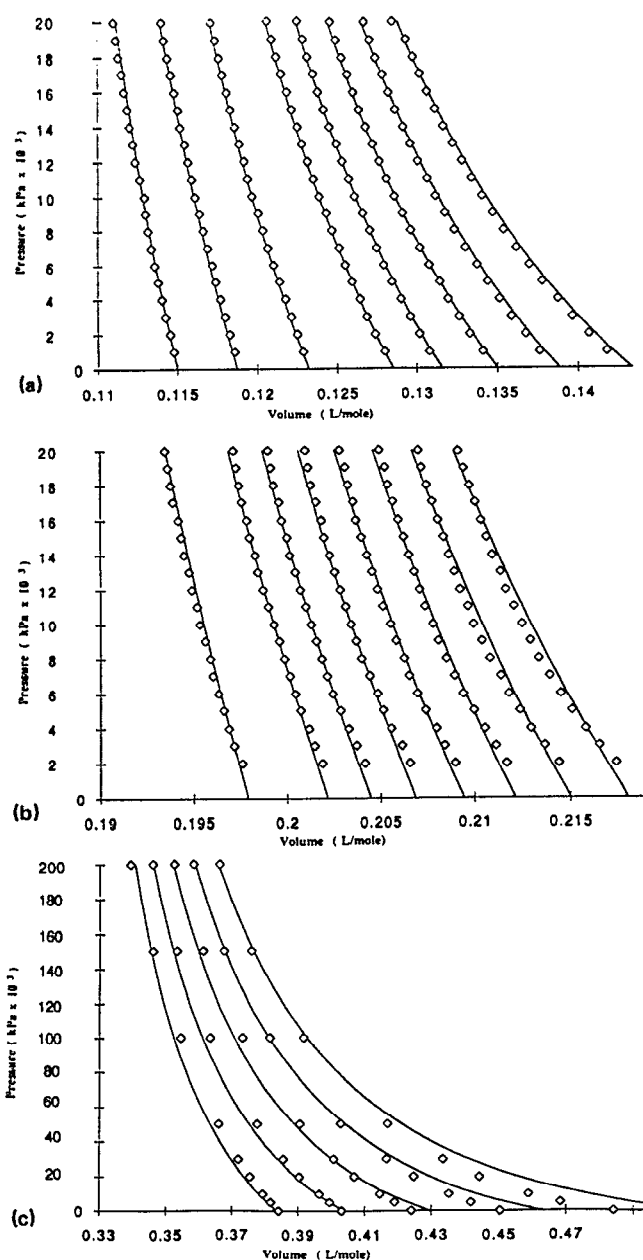


FIG. 1. BGY fit to experimental data (open symbols). (a) *n*-C5, isotherms are for  $T = 293, 313, 333, 353, 363, 373, 383, 393$  K; (b) *n*-C10, isotherms for the same set of temperatures as in (a); (c) *n*-C20, isotherms are for  $T = 373, 423, 473, 523, 573$  K.

The fits were done using a series of  $z$  values between 6 and 12; the effect of changing  $z$  is discussed later in this section. The best fit was considered to be that which minimized the chi square function<sup>18</sup>

$$\chi^2 = \sum_{i=1}^n \left[ \frac{P(V_i, T_i, \mathbf{a}) - P_i}{\sigma_i} \right]^2, \quad (21)$$

where  $P(V_i, T_i, \mathbf{a})$  represents the calculated value of  $P$  using independent variables  $V_i$  and  $T_i$ , and parameters  $r$ ,  $v$ , and  $\epsilon$  are represented by the vector  $\mathbf{a}$ ;  $P_i$  is the experimental value for the pressure at  $T_i$  and  $V_i$ .  $\sigma_i$  is the measurement uncer-

tainty for the  $i$ th data point, which was taken here to be a constant (in fact, one). In order to compare fits on different data sets (in particular, having pressure ranges which differed by an order of magnitude or more) a reduced chi parameter was developed, analogous to the coefficient of variation used in one-dimensional statistics

$$\chi_r = \frac{[\chi^2/(n-3)]^{1/2}}{(\sum_{i=1}^n P_i)/n}. \quad (22)$$

This merit function ranged from 0.03 to 0.20 for excellent to good fits. For the *n*-alkanes we used data sets at both high (between 20 and 200 MPa) and low (20 MPa or less) pressure.<sup>19</sup> Table I summarizes the fit parameters and  $\chi_r$  values for the *n*-alkane series. Looking at Fig. 1, it can be seen that BGY works extremely well for *n*-C5, and quite well for *n*-C10 and *n*-C20. Since fit results using the PV equation of state<sup>8</sup> were only available for *n*-C5 and *n*-C7 among the linear alkanes we shall focus on *n*-C5 in comparing BGY with other equations of state.

Consider first the fit parameters and the  $z$  dependence of the fit, as a function of the alkane chain length. Two combinations of the fit parameters are particularly suited to illustrate the effect of chain length:  $r\nu$ , the hard-core volume per molecule, and  $qz\epsilon$ , the interchain interaction energy associated with the maximum number of (nonbonded) nearest-neighbor contacts per chain. Figure 2 shows these quantities plotted against the number of carbons per molecule for different values of  $z$ . Figure 2(a) illustrates the excellent correlation between the hard core volume and the chain length; note that changing the lattice coordination number between 6 and 12 has no effect on these results. The hard-core volumes calculated here correlate well with values of the van der Waals  $b$  constant; for *n*-C4 to *n*-C10  $r\nu$  ranged from 58% to 64% of  $b$ .<sup>20</sup> The insensitivity to choice of  $z$ , and linear correlation with number of carbons are also visible in Fig. 2(b) where  $qz\epsilon$  is plotted; the negative slope of the plot is due to the fact that the nearest-neighbor interaction energies are negative. While  $qz\epsilon$  varies with the number of carbons, the energy density  $\epsilon/\nu$  stays reasonably constant throughout the series; the average is  $166 \pm 14.3$  J/mL. For the same subset of *n*-alkanes discussed above (*n*-C4 to *n*-C10) these energy

TABLE I. Results from BGY fit to data on *n*-alkanes.

Alkane	$r$	$\nu$ (mL/mol)	$\epsilon$ (J/mol)	$\chi_r$
<i>n</i> -C4	9.378	8.335	-1324	0.078 24
<i>n</i> -C5	12.07	7.747	-1379	0.044 78
<i>n</i> -C6	11.11	10.04	-1534	0.071 77
<i>n</i> -C7	13.64	8.983	-1468	0.156 4
<i>n</i> -C8	11.25	12.81	-1715	0.085 58
<i>n</i> -C9	16.51	9.236	-1532	0.170 8
<i>n</i> -C10	19.82	8.484	-1586	.060 13
<i>n</i> -C11	19.86	9.177	-1576	0.173 1
<i>n</i> -C13	22.22	9.569	-1628	0.195 4
<i>n</i> -C17	28.65	9.554	-1698	0.126 8
<i>n</i> -C20	30.95	10.42	-1780	0.111 1

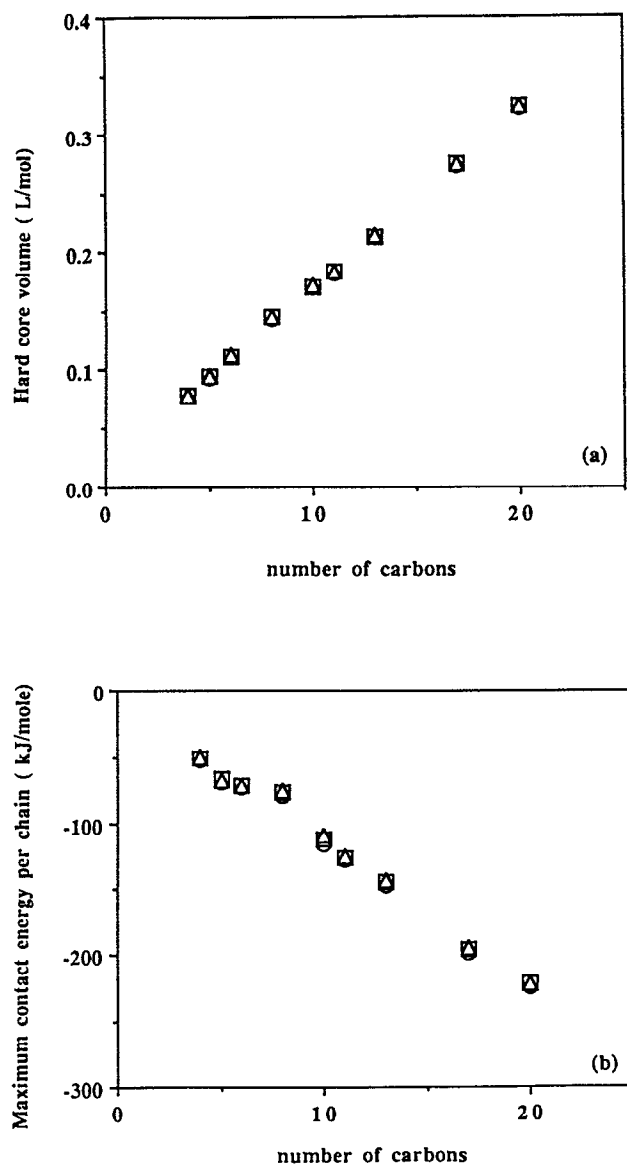


FIG. 2. Dependence on the alkane chain length of (a)  $rv$  and (b)  $qze$ .  $\circ$   $z = 6$ ;  $\square$   $z = 9$ ;  $\triangle$   $z = 11$ .

densities ranged from 50%–100% of the cohesive energy density<sup>21</sup> for the alkane of interest.

Figure 3 shows fits to the PVT data to three isotherms (293, 353, and 393 K) of the data for  $n$ -C5 using the LF<sup>5</sup> and PV<sup>8</sup> equations of state [Eqs. (13) and (14), respectively]; these should be compared with the BGY result, shown in Fig. 1(a). There are many equations of state which have been used successfully in fitting PVT data on small molecules; these two treatments were chosen because of their relationship to the BGY result, as discussed in Sec. II. Both the PV and LF results were plotted using parameters obtained from the literature. The BGY description comes the closest to the experimental data over the whole temperature range. Both PV and LF do reasonably well at 20 °C, while by 80 °C both are rather far off.

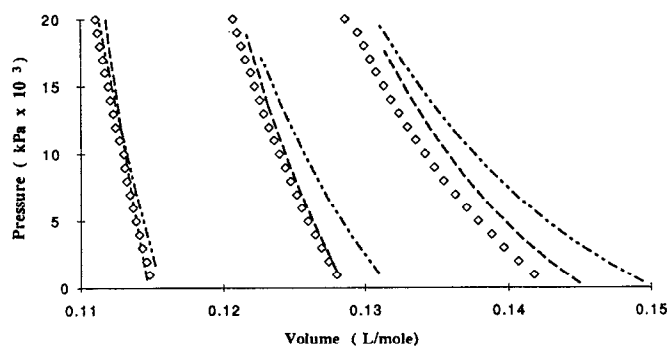


FIG. 3. Fit to experimental data on  $n$ -C5 using PV---and LF---. Isotherms are for  $T = 293, 353, 393$  K.

Thus far, the focus has been on the liquid state. Is BGY capable of predicting a phase transition? If so, how well can it do at estimating the critical point? Figure 4 answers one of these questions: Using the fit parameters obtained through a fit of the liquid state data for  $n$ -C5, a series of isotherms were generated which indicate the presence of a critical point ( $T_c$ ,  $V_c$ ,  $P_c$ ) and, below that, a two-phase region showing a van der Waals-type loop. The liquid–vapor coexistence curve can be mapped out by using an equal-area construction to identify the molar volumes of the gas and liquid in equilibrium below  $T_c$ . A plot of the predicted molar volumes for  $n$ -C5 as a function of temperature is shown in Fig. 5(a), which also includes the experimental results. Since the BGY fit was to the liquid data it is no surprise to see the theoretical curve fall right on those data points; the correlation with the vapor data, however, is very good as well. Figure 5(b), a plot of the predicted vapor pressure for  $n$ -C5 as a function of temperature, also shows how well the BGY treatment does at describing the vapor phase. The agreement with experiment is excellent over the range of temperatures, although it does appear that the two are closer at lower temperatures. In fact, the percent deviation from the experimental results is reduced as  $T_c$  is approached; this can be illustrated by a semi-log plot of  $P$  vs  $T$ , which is not shown.

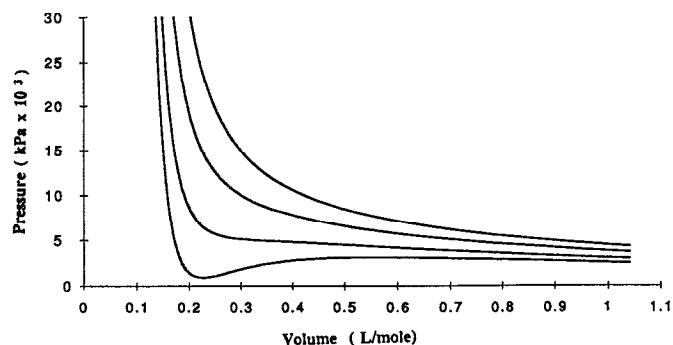


FIG. 4. A series of isotherms for  $n$ -C5 using the parameters obtained from the fit of liquid PVT data. The temperatures (from top to bottom): 600, 550, 490, 450 (K).

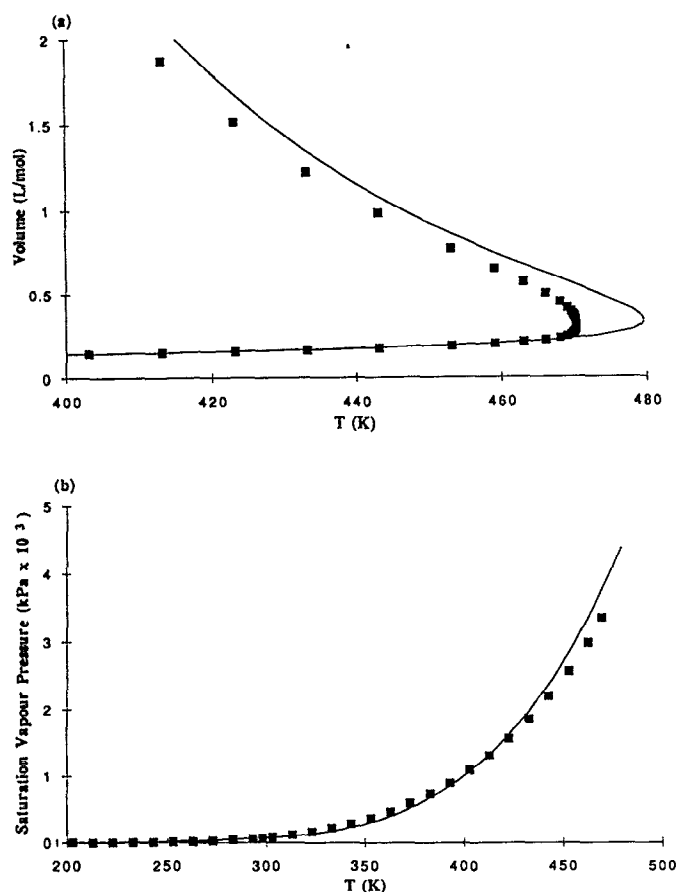


FIG. 5. (a) Molar volume of  $n$ -C5 vs temperature. (b) Saturation vapor pressure of  $n$ -C5 vs temperature. The solid line is the BGY prediction and the filled squares are from experimental data.

From Figs. 4 and 5 it can be seen that there is some disagreement between the predicted and experimental values of the critical point for  $n$ -C5. In fact, considering that the description is almost certainly a mean field one, BGY does remarkably well at predicting the critical points for the series of  $n$ -alkanes. This is illustrated in Fig. 6 in which the theo-

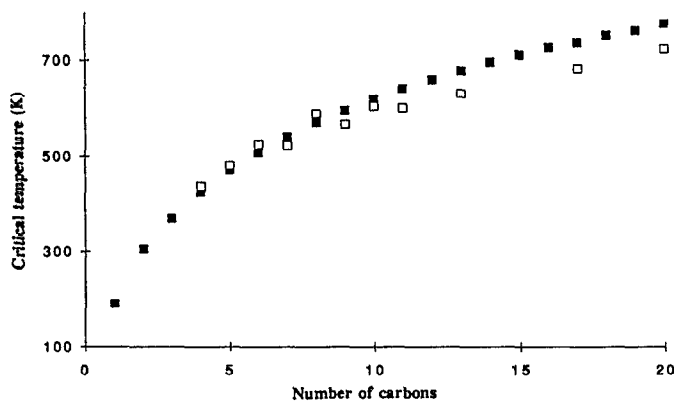


FIG. 6. A comparison of the predicted (open squares) and experimentally determined (filled squares) critical temperatures of the  $n$ -alkanes.

retical predictions for  $T_c$  are compared with the experimental results for  $n$ -C4 to  $n$ -C20. The BGY predictions are in excellent agreement with the experimental results although they tend to be a little high for  $n$ -alkanes associated with the low-pressure data, and are a bit below the experimental results for the cases in which high-pressure data were used.

Finally, for some of the  $n$ -alkanes the fit parameters were used to look at derivatives of the PVT surface. Figure 7 shows the isothermal compressibility,  $\kappa$ , as a function of pressure for a series of temperatures for  $n$ -C5.  $\kappa$  is defined as

$$\kappa = -\frac{1}{V} \left( \frac{\partial V}{\partial P} \right)_T. \quad (23)$$

The agreement between the BGY predictions and the experimental results is good throughout, and is excellent in the middle range of temperatures. This trend is also seen for the related derivatives  $\alpha$  (the thermal expansion coefficient), and  $\gamma$  (the thermal pressure coefficient).

Next, we shall consider data on three polymeric systems, all in the melt phase: polystyrene (PS),<sup>22</sup> poly(orthomethylstyrene) (PoMS),<sup>23</sup> and poly(vinylacetate) (PVAc).<sup>24</sup> The fit parameters are listed in Table II. For the polymer data  $r'$  and  $q'$  were used, where  $r' = r/M_0$  and  $q' = q/M_0$ .  $M_0$  is the mass associated with the portion of the chain occupying one lattice site. Using  $r'$ ,  $q'$ , and the specific (instead of the molar) volume leave Eq. (9) unchanged in form, and allows us to fit the experimental data without having to specify a molar mass for the polymer. Figure 8(a) shows the PVT fits to data on polystyrene, over a temperature ranging from 373 to 504 K, with the three isotherms at 422, 463, and 504 K highlighted. The BGY fit is very good, although it overestimates the curvature of the isotherms a little at the higher temperatures. In Fig. 8(b) the BGY fits for the three isotherms highlighted in Fig. 8(a) are compared with those fits obtained using the LF, LC, and SS equations. For these data all of the fits were done by us, using the approach outlined in Sec. IV; the fit parameters are given

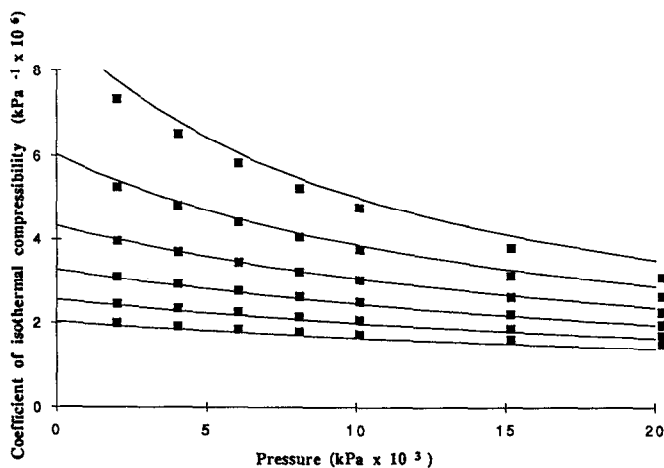


FIG. 7. A comparison of the predicted (solid curves) and experimentally determined (filled squares) coefficient of isothermal compressibility of  $n$ -C5, as a function of pressure. The isotherms range from 293 to 393 K (top to bottom) in increments of 20 K.

TABLE II. Results from fits to PVT data on polymers.

	$r^*$	$v$ (mL/mol)	$\epsilon$ (J/mol)	$\chi_r$
Polystyrene				
BGY	102.7	8.472	-2126	0.040 46
LC	76.10	11.76	1896	0.080 88
PV <sup>b</sup> : $\epsilon = 848.1 + T(0.5479)$ (J/mol), $v^* = rv = 0.8803$ (mL/g); $\chi_r = 0.048 88$				
LF <sup>c</sup> : $T^* = 689.3$ (K), $P^* = 425.8$ (MPa), $\rho^* = 1.120$ (g/mL); $\chi_r = 0.058 28$				
SS (cell) <sup>d</sup> : $T^* = 4858$ (K); $V^* = 0.9044$ (mL/g); $P^* = 666.5$ (MPa); $\chi_r = 0.019 99$				
Poly(orthomethylstyrene)				
BGY	92.61	9.655	-2267	0.045 53
LC	72.48	12.63	1989	0.099 55
PV: $\epsilon = 764.0 + T(0.8494)$ (J/mol), $v^* = rv = 0.9000$ (mL/g); $\chi_r = 0.066 54$				
LF: $T^* = 768.0$ (K), $P^* = 379.0$ (MPa), $\rho^* = 1.079$ (g/mL); $\chi_r = 0.1432$				
SS (cell): $T^* = 5128$ (K); $V^* = 0.9280$ (mL/g); $P^* = 600.6$ (MPa); $\chi_r = 0.049 14$				
Poly(vinylacetate)				
BGY	136.4	5.498	-1732	.030 91
LC	91.30	8.566	1627	.069 80
PV: $\epsilon = 1000.0 + T(-0.029 29)$ (J/mol), $v^* = rv = 0.7850$ (mL/g); $\chi_r = 0.094 64$				
LF: $T^* = 590.0$ (K), $P^* = 508.7$ (MPa), $\rho^* = 1.283$ (g/mL); $\chi_r = 0.072 81$				
SS (cell): $T^* = 3782$ (K); $V^* = 0.7731$ (mL/g); $P^* = 756.6$ (MPa); $\chi_r = 0.012 47$				

<sup>a</sup>For the fits to the data on polymers Eq. (9) was rewritten in terms of specific (not molar) volumes, and  $r' = r/M_0$  and  $q' = q/M_0$  were used in place of  $r$  and  $q$ , where  $M_0$  represents the mass of chain occupying a lattice segment.

<sup>b</sup>See Ref. 8; the authors fixed volume per lattice site at 9.75 mL/mol. Note opposite sign convention for  $\epsilon$ .

<sup>c</sup>See Ref. 5 for both definitions and values of these parameters for PoMS and PVAc.

<sup>d</sup>See Ref. 9 for both definitions and values of parameters for PoMS and PVAc;  $r/3c$  is set to equal one.

in Table II. The SS equation of state does the best job of fitting over the entire range of molar volumes, particularly at higher temperatures. However, looking, for example, at the low-pressure portion of the isotherm at 504 K, it can be seen that the BGY curve comes next, closely followed in this case by PV, then SL and LC.

Figures 9 and 10 are analogous to Fig. 8 in that the BGY fits are shown in part a, with the results using other equations of state illustrated in part b. For these cases only the BGY and LC fits were done by us; the other fits shown were plotted using parameters obtained in the literature for the relevant data sets (see Table II). In Fig. 9 the polymer of interest is poly(ortho-methylstyrene), and in Fig. 10 it is poly(vinylacetate). In both cases BGY does a very good job at fitting the PVT data over a wide range of temperatures. Indeed, as was seen in Fig. 8, only SS does a consistently better job at describing the experimental results. Note that although the BGY and PV fits were very close for the polystyrene data, BGY is distinctly better for the lowest-temperature isotherm in Fig. 10(b) for poly(vinylacetate).

In Fig. 11 we compare the BGY prediction for  $\alpha$ , the thermal expansion coefficient, with experimental results for poly(vinylacetate)<sup>24</sup> over pressure ranging from one to 80 MPa.  $\alpha$  is defined as

$$\alpha = \frac{1}{V} \left( \frac{\partial V}{\partial T} \right)_P \quad (24)$$

The BGY prediction is within  $\pm 8\%$  of the experimental result over this range in pressure. The best agreement with experimental data is in the middle of the pressure range, as noted in the analysis of the results for *n*-pentane, discussed above.

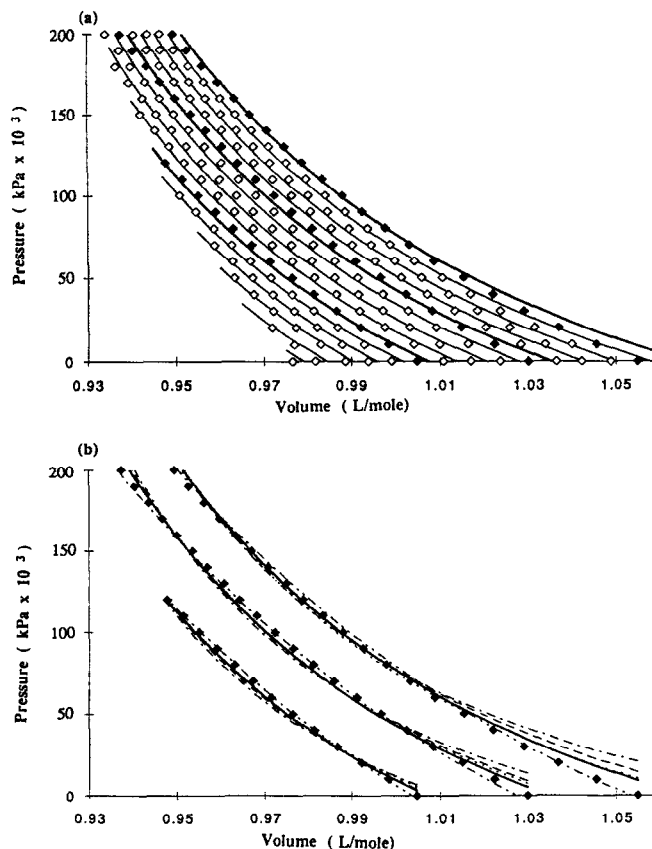


FIG. 8. Fit to experimental PVT data on polystyrene (Ref. 22) (symbols). (a) BGY fits to a series of isotherms ranging from 373.65 to 503.65 K (left to right), with the highlighted temperatures 422.15, 463.45, and 503.65 K. (b) Fits to the three isotherms highlighted in (a) using:—BGY; ---LC; ···PV; -·-LF; - - -SS.

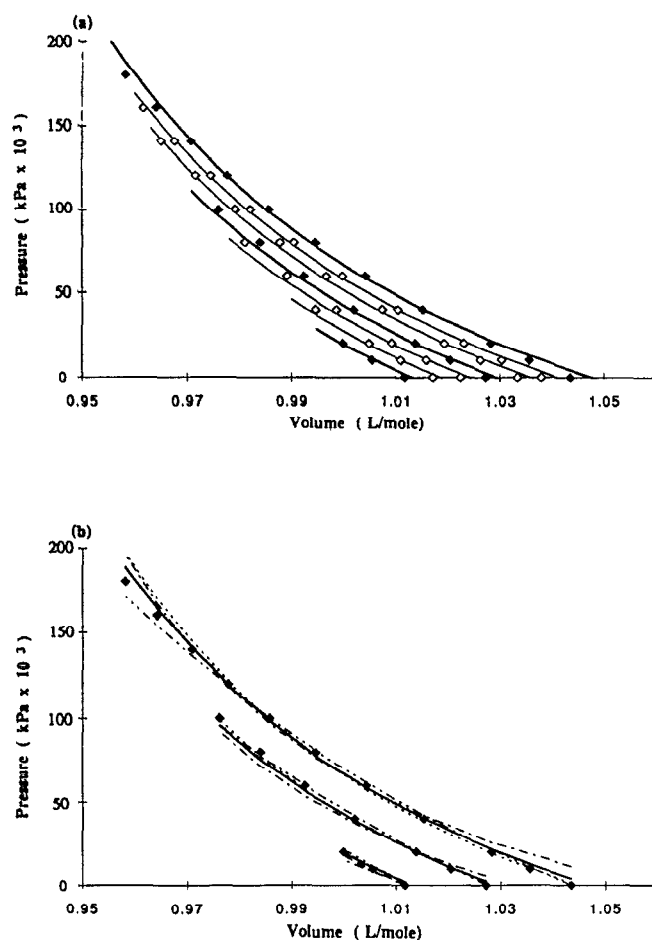


FIG. 9. Fits to PVT data on poly(orthomethylstyrene) (Ref. 23); same notation as Fig. 8. The isotherms span the range 412.55 to 470.85 K; the temperatures highlighted in (a) and featured in (b) are: 412.55, 441.25, and 470.85 K.

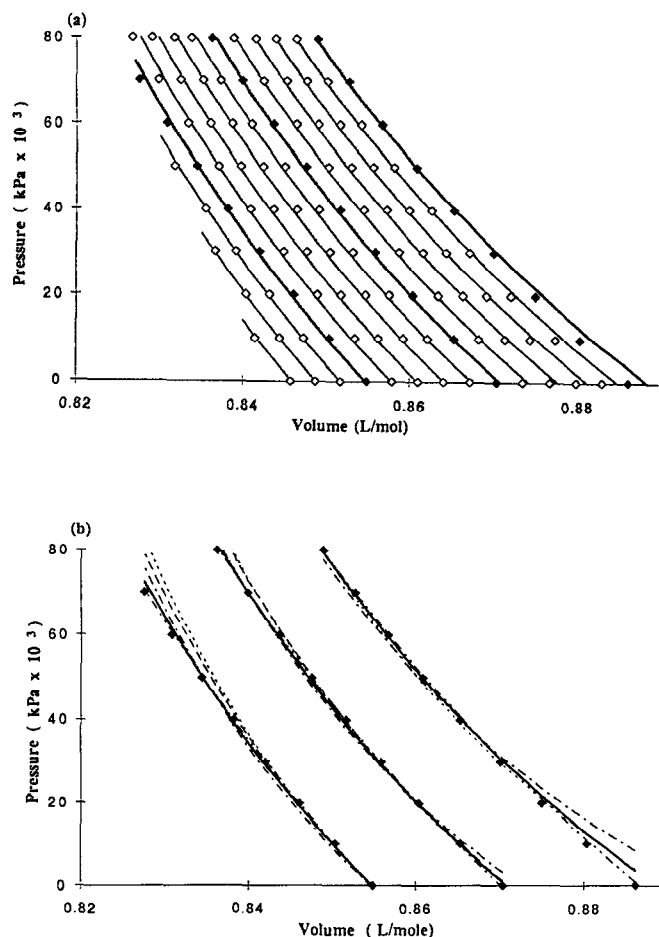


FIG. 10. Fits to PVT data on poly(vinylacetate) (Ref. 24); same notation as Fig. 8. The isotherms span the range 308.15 to 373.15 K; the temperatures highlighted in (a) and featured in (b) are: 323.15, 348.15, and 373.15 K.

Although the data are not shown in Table II we also fitted the BGY equation to PVT data for the glassy state of the polymers studied. In all cases,  $r'$  was larger for the melt than for the glass of a particular polymer; this can be understood by recalling that  $r'$  is proportional to the number of freely jointed connected segments per chain. This number should be greater for the melt, reflecting the greater flexibility of chains above the glass transition. Since the hard-core volume of the chain should be independent of whether it is the molten or glassy state,  $\nu$  must therefore decrease in going from a melt to a glass, and that is what was found; the product  $r'\nu$  changed less than 5%.

In all, it would seem that each of the equations of state used is capable of providing at least a reasonable fit to fluid PVT data. For *n*-C5 BGY appears to do significantly better than either PV or LF. For the polymeric systems all of the equations used did a good job. Niess and Stroeks<sup>25</sup> have commented recently that two descriptions which appear to do equally well at fitting liquid PVT data can differ significantly in other ways, e.g., in predictions regarding phase separation behavior in mixtures. Thus, even though the numerous equations used did an apparently similar job in de-

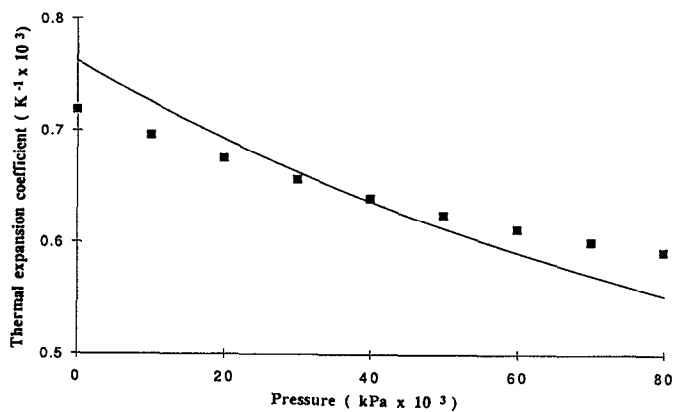


FIG. 11. A comparison of the predicted (solid line) and experimentally determined (filled symbols) thermal expansion coefficient as a function of pressure for poly(vinylacetate).



scribing the polymeric PVT surface, it remains to be seen how they will differ when used to treat mixtures of, for example, polymeric fluids.

## VI. CONCLUSIONS

In this work we have extended our studies using the BGY integral equation treatment to include the case of a compressible pure fluid. We have commented on how well the BGY predictions for the athermal fluid (GRM) compare with lattice Monte Carlo results as well as with the FH and LC predictions for the athermal case. In addition, we have studied a series of *n*-alkanes (a selection from *n*-C4 to *n*-C20) as well as three different polymeric fluids [polystyrene, poly(orthomethylstyrene), and poly(vinylacetate)], comparing the BGY fits and predictions with those from theories including the LC, LF, PV, and SS treatments. In all of these cases the BGY approach does very well, showing that it is indeed capable of describing fluid PVT results and predicting thermodynamic properties, both for the liquid and (where appropriate) gas phases.

In Sec. IV we referred to continuum Monte Carlo results for athermal chains. Dickman and Hall<sup>11</sup> have pointed out, in determining the pressure for such systems, that the lattice and continuum results are dramatically different, and that the lattice models (such as FH or GRM) do very poorly at describing the continuum results.<sup>26</sup> Here we have noted the excellent agreement between GRM and the lattice Monte Carlo results, and then have continued using our lattice model to fit experimental data, which means applying a lattice version of BGY to describe continuum systems. How can this be justified? We have seen that the lattice version of the equation of state does very well indeed at fitting the continuum PVT data. Shall our defense be that "it works?" The conclusion might then be that any reasonable form of the equation of state with three fitting parameters is sufficient. However, the BGY approach must be doing a good job at describing the underlying physical behavior, since the fits of liquid data lead to accurate predictions on properties of the vapor and good estimates of the critical points. Thus, while the lattice version of BGY may not be quantitatively correct, in the sense that when there are no adjustable parameters it does poorly with respect to simulation results for quantities such as pressure or the compressibility factor, it must get the physics of the system qualitatively correct. Hence it would seem that the lattice description is rather robust, and that the flexibility afforded by having three parameters makes up the difference between being qualitatively and quantitatively right. Since we are currently studying the continuum analog of this problem using BGY, we will soon be able to report on the differences in using the lattice and continuum versions of the same theoretical approach.

Our goal here was to show that the BGY theory is effective at describing a one-component compressible system. We are now in a position to investigate compressible mixtures, and this work is currently in progress.

## ACKNOWLEDGMENTS

J. E. G. L. most gratefully acknowledges the support of the donors of the Petroleum Research Fund, administered

by the American Chemical Society. In addition, the authors wish to thank D. J. Walsh for supplying PVT data on polystyrene.

- <sup>1</sup> J. E. G. Lipson, *Macromolecules* **24**, 1334 (1991).
- <sup>2</sup> J. E. G. Lipson, *J. Chem. Phys.* **96**, 1418 (1992).
- <sup>3</sup> E. A. Guggenheim, *Proc. R. Soc. London, Ser. A* **183**, 203, 213 (1944).
- <sup>4</sup> H. Tompa, *Polymer Solutions* (Academic, New York, 1956).
- <sup>5</sup> (a) I. C. Sanchez and R. H. Lacombe, *Macromolecules* **11**, 1145 (1978); (b) *J. Polym. Sci., Polym. Lett. Ed.* **15**, 71 (1977).
- <sup>6</sup> J. Dudowicz, K. F. Freed, and W. G. Madden, *Macromolecules* **23**, 1181 (1990), and references cited therein.
- <sup>7</sup> M. G. Bawendi and K. F. Freed, *J. Chem. Phys.* **88**, 2741 (1988).
- <sup>8</sup> C. Panayiotou and J. H. Vera, *Polym. J.* **14**, 681 (1982).
- <sup>9</sup> (a) R. Simha and T. Somcynsky, *Macromolecules* **2**, 342 (1969); (b) J. E. McKinney and R. Simha, *Macromolecules* **7**, 894 (1974).
- <sup>10</sup> R. Dickman and C. K. Hall, *J. Chem. Phys.* **85**, 3023 (1986).
- <sup>11</sup> R. Dickman and C. K. Hall, *J. Chem. Phys.* **85**, 4108 (1986).
- <sup>12</sup> K. G. Honnell and C. K. Hall, *J. Chem. Phys.* **90**, 1841 (1989).
- <sup>13</sup> (a) A. Hertanto and R. Dickman, *J. Chem. Phys.* **89**, 7577 (1988); (b) *ibid.* **93**, 774 (1990).
- <sup>14</sup> Equation (3.26) from Ref. 7 is

$$\begin{aligned} (l/r) \ln p_{l,c}(\phi, r) = & \ln(1 - \phi) + (2\phi/z) [(r-1)/r]^2 + (2\phi/z^2 r^4) \\ & \times [3(r-1)^4 - 8(r-1)^2 - 4(r-1) + 1] \\ & - (2\phi^2/z^2 r^4) [5(r-1)^4 - (r-1)^3 - 6(r-1)^2] \\ & + (8\phi^3/z^2) [(r-1)/r]^4 + O(z^{-3}). \end{aligned}$$

Note that what is called GRM here is called HMG (Huggins-Miller-Guggenheim) in Ref. 7.

<sup>15</sup> For example, the work in Ref. 2 showed that for nonathermal incompressible lattice mixtures BGY and LC yielded similar predictions with respect to thermodynamic properties ( $\Delta E_{\text{mix}}$ ,  $\Delta S_{\text{mix}}$ ) for the polymer-solvent and polymer blend cases.

<sup>16</sup> Equation (3.31) from Ref. 7 is

$$\begin{aligned} \omega_{l,c} = \omega_{\text{FH}} - \phi \left\{ \frac{(r-1)^2}{zr} + \frac{3(r-1)^4 - 8(r-1)^2 - 4(r-1) + 1}{z^2 r^3} \right\} \\ - \phi^2 \left\{ \frac{-20(r-1)^4 + 4(r-1)^3 + 24(r-1)^2}{3z^2 r^3} \right\} \\ - \phi^3 \left\{ \frac{6(r-1)^4}{z^2 r^3} \right\} + O(z^{-3}). \end{aligned}$$

- <sup>17</sup> N. B. Vargaftik, *Tables on the Thermophysical Properties of Liquids and Gases*, 2nd ed. (Wiley, New York, 1975).
- <sup>18</sup> W. H. Press, B. P. Flannery, S. A. Teukolsky, and W. T. Vetterling, *Numerical Recipes* (Cambridge University, Cambridge, 1989).
- <sup>19</sup> High pressure data were used for: *n*-C7, *n*-C9, *n*-C11, *n*-C13, *n*-C17, *n*-C20. We typically omitted the two highest-pressure data points.
- <sup>20</sup> *Handbook of Chemistry and Physics* (CRC, Boca Raton, 1988).
- <sup>21</sup> *Polymer Handbook*, 2nd ed., edited by J. Brandrup and E. H. Immergut (Wiley, New York, 1975).
- <sup>22</sup> The PVT data for polystyrene were obtained courtesy of Dr. D. J. Walsh, Du Pont et Nemours.
- <sup>23</sup> A. Quach and R. Simha, *J. Appl. Phys.* **42**, 4592 (1971).
- <sup>24</sup> J. E. McKinney and M. Goldstein, *J. Res. Natl. Bur. Stand. A* **78**, 331 (1974).
- <sup>25</sup> E. Nies and A. Stroeks, *Macromolecules* **23**, 4092 (1990).
- <sup>26</sup> In fact, these authors developed a continuum analog of GRM which they referred to as "Generalized Flory-Huggins," GFH. Figures 2-4 of Ref. 11 show that GFH did extremely well in comparison with MC results in two and three dimensions. When we have extended our BGY treatment to the continuum it will be interesting to see how our athermal theory does; at this point we shall also be able to compare our description with that of J. G. Curro and K. S. Schweizer [see, for example, the paper by these authors in *J. Chem. Phys.* **89**, 3350 (1988)].